AD-A031 895 CALIFORNIA UNIV BERKELEY DEPT OF PHYSICS F/G 20/12
PARAMETRIC AMPLIFICATION AND OSCILLATION AT 36 GHZ USING A POIN--ETC(U)
NOV 76 Y TAUR, P L RICHARDS N00014-75-C-0496

UNCLASSIFIED NL

| OF |

AD
A031895

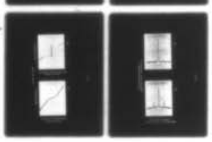

END

DATE
FILMED
1 — 77

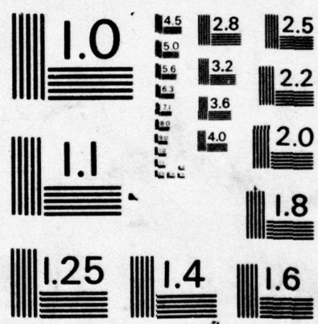

MICROCOPY RESOLUTION TEST CHART

NATIONAL BUREAU OF STANDARDS-1963-A

ADA031895

(12)

SECURITY CLASSIFICATION OF THIS PAGE (When Data Entered)

REPORT DOCUMENTATION PAGE		READ INSTRUCTIONS BEFORE COMPLETING FORM
1. REPORT NUMBER	2. GOVT ACCESSION NO.	3. RECIPIENT'S CATALOG NUMBER
(9) Technical Rept. 1 Feb 76-31 Jan 77		
4. TITLE (and Subtitle) (6) PARAMETRIC AMPLIFICATION AND OSCILLATION AT 36 GHz USING A POINT CONTACT JOSEPHSON JUNCTION.		5. TYPE OF REPORT & PERIOD COVERED Technical - 2/1/76 to 1/31/77
		6. PERFORMING ORG. REPORT NUMBER
7. AUTHOR(s) (10) Y. Taur and P. L. Richards		8. CONTRACT OR GRANT NUMBER(s) (15) NØ0014-75-C-0496
9. PERFORMING ORGANIZATION NAME AND ADDRESS Professor P. L. Richards Department of Physics University of California, Berkeley, Calif. 94720		10. PROGRAM ELEMENT, PROJECT, TASK AREA & WORK UNIT NUMBERS NR 319-055
11. CONTROLLING OFFICE NAME AND ADDRESS Office of Naval Research Physics Program Office Arlington, Virginia 22217		12. REPORT DATE (11) Nov 76
		13. NUMBER OF PAGES 27 (12) 28p.
14. MONITORING AGENCY NAME & ADDRESS (if different from Controlling Office)		15. SECURITY CLASS. (of this report) Unclassified
		15a. DECLASSIFICATION/DOWNGRADING SCHEDULE

16. DISTRIBUTION STATEMENT (of this Report)

Unlimited

DISTRIBUTION STATEMENT A
Approved for public release;
Distribution Unlimited

17. DISTRIBUTION STATEMENT (of the abstract entered in Block 20, if different from Report)

18. SUPPLEMENTARY NOTES

To be published in Journal of Applied Physics

19. KEY WORDS (Continue on reverse side if necessary and identify by block number)

Superconductivity, Josephson effect, parametric amplifier

20. ABSTRACT (Continue on reverse side if necessary and identify by block number)

We have observed doubly degenerate parametric amplification and oscillation at 36 GHz from a single point contact Josephson junction. The experimental results agree qualitatively with theoretical calculations based on the resistively shunted junction model. The estimated noise temperature of an amplifier with 11 dB net gain is consistent with zero, but has an upper limit of 50 K. Attempts to observe parametric amplification in the singly degenerate mode with a pump frequency of 72 GHz were not successful.

DD FORM 1 JAN 73 1473 EDITION OF 1 NOV 65 IS OBSOLETE
S/N 0102-LF-014-6601

071 970

SECURITY CLASSIFICATION OF THIS PAGE (When Data Entered)

To be published in J. Appl. Phys.

PARAMETRIC AMPLIFICATION AND OSCILLATION AT 36 GHz USING A POINT CONTACT JOSEPHSON JUNCTION*

Y. Taur† and P. L. Richards

Department of Physics
University of California
Berkeley, California 94720

ABSTRACT

We have observed *doubly degenerate* parametric amplification and oscillation at 36 GHz from a single point contact Josephson junction. The experimental results agree qualitatively with theoretical calculations based on the resistively shunted junction model. The estimated noise temperature of an amplifier with 11 dB net gain is consistent with zero, but has an upper limit of 50 K. Attempts to observe parametric amplification in the singly degenerate mode with a pump frequency of 72 GHz were not successful.

I. INTRODUCTION

Because of their nonlinear electrical properties at microwave frequencies, Josephson junctions are being investigated for operation in such devices as video detectors,[1-3] heterodyne mixers,[4,5] and parametric amplifiers.[6,7] In some of these applications the junction is dc biased at finite voltage so that Josephson oscillations take place. In this way a Josephson junction can, for example, be operated as a self-pumped parametric amplifier.[6,8,9] Alternatively, a Josephson junction can be operated with zero dc voltage bias so that it behaves as a nonlinear inductor for currents less than the critical current I_c. Early theoretical calculations[7,10,11] suggested that junctions biased in this way could be operated as a three photon parametric device with an external pump at the sum of the signal and idler frequencies $\omega_p = \omega_s + \omega_i$ or as a four photon device with $2\omega_p = \omega_s + \omega_i$.

The singly degenerate mode of three photon operation $(\omega_p \simeq 2\omega_s \simeq 2\omega_i)$ was first explored for the case of a parametric excitation of the plasma oscillation in a Josephson tunnel junction which was pumped by an rf current source at twice the plasma frequency and dc biased with $0<I<I_c$. This effect was discovered with an analog junction simulator,[10] the threshold has been calculated analytically in the small signal limit,[11] and indirectly verified with thin film tunnel junctions.[12]

A series array of Dayem bridges with no dc bias has been operated in the doubly degenerate four photon mode $(\omega_p \simeq \omega_s \simeq \omega_i)$ as a parametric amplifier at 9 and 33 GHz.[7] This is an attractive device with significant gain,

wide bandwidth, and low noise temperature.

In order to observe parametric effects it is necessary to minimize parasitic power loss due to currents which flow at the harmonics and combinations of ω_p, ω_s and ω_i. In the case of the singly degenerate device which uses a current biased thin film tunnel junction, these currents remain inside the junction and, especially at high frequencies, the shunt capacitance shorts out the lossy quasiparticle conductance. In the doubly degenerate device[7] parasitic currents at frequencies $\ell\omega_p+m\omega_s$ vanish by symmetry when $\ell + m$ is an even interger. Because the impedance of the series array of junctions used for these experiments was relatively high, it was possible to use transmission line techniques to short out currents for $\ell + m = 3$, so that the lowest parasitic frequencies at which loss occurred were in the neighborhood of $5\omega_p$.

In this paper we report a study of parametric amplification by a single point contact Josephson junction with zero dc bias voltage. The junction was mounted in a Ka-band waveguide cavity as is shown in Fig. 1. The signal and idler frequencies ω_s and ω_i lay within the bandwidth of the cavity resonance at 36 GHz. Pump power was applied from external sources at $\omega_p/2\pi \sim 72$ GHz (the singly degenerate 3 photon mode) and at ~36 GHz (the doubly degenerate 4 photon mode).

Niobium point contact junctions were used whose dc I-V characteristics, rf properties and noise have been found to be in good agreement with the resistively shunted junction model for the frequencies employed.[5,13] The equivalent circuit of such a junction in the resonant cavity is shown in Fig. 2. The circuit elements representing

wire inductance and cavity loss make this device differ in a significant way from those mentioned above. During the experiments the plunger capacitance was adjusted so that the cavity resonated at $\omega_p/2$ for the 3 photon case and at ω_p for the four photon case. Since the junction resistance R is small compared with the impedance coupled to the junction at harmonic frequencies, we believe that the only significant Fourier components of current external to the junction are at ω_p, ω_s and ω_i. This is not as favorable a termination of the harmonic and combination frequencies as was achieved in the devices mentioned above since, in our case, internal parasitic currents still occur which cause dissipation in the quasiparticle resistance R.

The experimental results for the 3 photon singly degenerate mode of operation occasionally showed a small response at the idler frequency, but never parametric gain. This was in sharp contrast to our results for the four photon doubly degenerate case. These usually gave large idler response which was often accompanied by significant gain.

This result is in disagreement with the result of an analytical calculation based on the current biased tunnel junction circuit model which predicts a lower threshold for the three photon mode.[14] A number of factors of practical importance contribute to this discrepancy. The analytical calculation is valid only in the small pump limit. In practice the amplification threshold can be reached in this limit only if external circuit loss is negligible. The higher order doubly degenerate process is relatively more effective at the higher pump power levels used in our experiments. Finally, the 3 photon process occurs only when the

junction is biased with a constant current which is a significant fraction of the critical current. It should therefore be more sensitive to the noise which causes the rounding of the I-V curve which was present in the experiments, but not in the analytical calculations.

Attempts were made to explore these ideas using the analog junction simulators which proved so useful in understanding our experiments with point contact heterodyne mixers.[5] These attempts were discontinued when it was discovered that the results obtained at zero dc voltage were sensitive to deviations from ideal behavior in both of our simulators.[15,16]

The remainder of this paper contains a detailed description of the results of our four photon doubly degnerate point contact amplifier experiments.

II. NUMERICAL CALCULATIONS

We make the assumption that the junction is looking into a very high microwave impedance except (for the four photon case) at ω_p, ω_s, and $\omega_i = 2\,\omega_p - \omega_s$. The current equation describing the junction response can then be written as

$$\frac{\hbar}{2eR}\frac{d\phi}{dt} + I_c \sin\phi = I_p \cos \omega_p t + I_s \cos(\omega_s t+\theta_s) + I_i \cos(\omega_i t+\theta_i), \quad (1)$$

where ϕ is the superconducting phase difference across the junction and $\frac{\hbar}{2e}\frac{d\phi}{dt}$ is the junction voltage according to the Josephson relations.

Since we are primarily interested in the limit in which the signal and idler currents are small, I_s, $I_i \ll I_p$, I_c, Eq. (1) can be separated into a nonlinear pump equation and a small signal linear equation by letting $\phi = \phi_o + \phi_1$ where $\phi_1 \ll \phi_o$:

$$\frac{\hbar}{2eR}\frac{d\phi_o}{dt} + I_c \sin\phi_o = I_p \cos \omega_p t \quad (2)$$

$$\frac{\hbar}{2eR}\frac{d\phi_1}{dt} + I_c \phi_1 \cos \phi_o = I_s \cos(\omega_s t+\theta_s) + I_i \cos(\omega_i t+\theta_i). \quad (3)$$

Equation (2) is similar to that considered in Ref. 10 for tunnel junctions except for the absence of the capacitance term. That theory (and its extension to the four photon case) is valid only if $I_p \ll I_c$. In order to obtain parametric gain in practice, one usually has to pump hard enough that $I_p \approx I_c$. We therefore used a digital computer to solve Eqs. (2) and (3) for the required cases.

Due to the symmetry of the unbiased junction $\phi_1(t)$ contains only the mixing products between the signal and the even harmonics of the pump that is ω_s, $2\omega_p \pm \omega_s$, $4\omega_p \pm \omega_s$, etc. Since ϕ_1 is linear in both I_s and I_i, we can evaluate the Fourier components of $\frac{\hbar}{2e}\frac{d\phi_1}{dt}$ at ω_s and ω_i (designated as V_s and V_i) and represent the junction by a complex 2x2 impedance matrix:[17]

$$\begin{bmatrix} V_s \\ V_i^* \end{bmatrix} = \begin{bmatrix} Z_{ss} & Z_{si}^* \\ Z_{is} & Z_{ii}^* \end{bmatrix} \begin{bmatrix} I_s \\ I_i^* \end{bmatrix} . \tag{4}$$

Both Z_{ss} and Z_{ii}^* have a positive real part from direct loss in the junction resistance R and an imaginary part from the linear component of the Josephson inductance. The cross terms Z_{si}^* and Z_{is}, which are responsible for the parametric negative resistance, arise from coupling between the signal and idler via the pump. There exists a common phase factor in both Z_{si} and Z_{is}.

Suppose the external termination at the idler frequency is Z_i so that $V_i^* + Z_i^* I_i^* = 0$. It is easy to show that the junction input impedance at the signal frequency is given by

$$Z_{in} = \frac{V_s}{I_s} = Z_{ss} - \frac{Z_{si}^* Z_{is}}{Z_i^* + Z_{ii}^*} . \tag{5}$$

For the degenerate case where $\omega_p = \omega_s = \omega_i$, $Z_{ss} = Z_{ii}$ and $Z_{si}^* Z_{is} = |Z_{si}|^2 > 0$. Then the real part of Z_{in} will be most negative if Z_i^* is adjusted such that it cancels the imaginary part of Z_{ii}^*, that is,

$Z_i^* + Z_{ii}^* = \mathrm{Re}\, Z_{ii} = \mathrm{Re}\, Z_{ss}$. Therefore,

$$\mathrm{Re}\, Z_{in} = \mathrm{Re}\, Z_{ss} - \frac{|Z_{si}|^2}{\mathrm{Re}\, Z_{ss}}, \tag{6}$$

which is negative if and only if $\mathrm{Re}\, Z_{ss} - |Z_{si}| < 0$. This result can easily be modified to include the effect of other losses in the cavity represented by R_L in series with the junction. The criterion for parametric amplification or oscillation is then

$$R_L + \mathrm{Re}\, Z_{ss} - |Z_{si}| < 0. \tag{7}$$

In order to obtain net gain from the junction, the negative resistance arising from parametric interaction must exceed both the direct loss in the junction and the external losses in the microwave cavity.

Although the actual negative resistance seen by the signal source depends on the details of the microwave arrangement, the quantity $\mathrm{Re}\, Z_{ss} - |Z_{si}|$ gives a limit on the allowed resistive loss in the cavity. We have solved for $\mathrm{Re}\, Z_{ss} - |Z_{si}|$ normalized by R as a function of normalized pump current I_p/I_c and normalized frequency $\Omega_p = \hbar\omega_p/2eRI_c$. The computed results are shown in Fig. 3 for three normalized frequencies. There are certain values of I_p at which both $\mathrm{Re}\, Z_{ss}$ and $|Z_{si}|$ go to infinity. Such divergences occur when the zero-voltage current is suppressed to zero and the solution $\phi_o(t)$ changes discontinuously from one branch to the other.[18] We are not particularly interested in such unbounded results since the presence of noise will undoubtedly smear out these singularities

in a real experiment. What is significant is that there exist regions where Re $Z_{ss} - |Z_{si}|$ is negative and finite, indicating the possibility for parametric gain. Figure 3 shows that such negative resistance regions become less negative as Ω_p increases. In fact, Re $Z_{ss} - |Z_{si}|$ is never negative if $\Omega_p \geq 0.3$. Such a degradation of the parametric process was expected since the Josephson element is more severely shorted by R at larger normalized frequencies. For $\Omega_p \ll 0.1$, on the other hand, the negative resistance persists for many periods. It would be difficult to use in practice, since both Z_{ss} and $|Z_{si}|$ change so rapidly with I_p that fluctuations in the pump current would prevent stable operation. Another general feature revealed by the calculation is that there is no negative parametric resistance when $I_p \gg I_c$. This can be explained in terms of saturation of the Josephson nonlinearity by the applied pump power.[19]

III. EXPERIMENTAL RESULTS

The experimental arrangement shown in Fig. 4 was set up so that the junction can function as a conventional reflection-type parametric amplifier utilizing a microwave circulator. The frequencies of the pump and signal klystrons were set about 10-20 MHz apart around 36.20 GHz. The reflected microwave power from the junction goes to a commercial resistive mixer with a third klystron to supply the local oscillator (LO) power. The frequency of the LO is usually set at 35.90 GHz so that the intermediate frequency (i.f.) for the signal is at 300 MHz. A spectrum analyzer (1-500 MHz) is used to display the reflected microwave spectrum on a scope. There are isolators between the circulator and mixer (total isolation > 100 dB, insertion loss = 2 dB) to prevent the LO power from reaching the junction. We also have a microwave short circuit which can be switched into the line to reflect the signal before it enters the cryostat. This provides a reference to measure the net gain of the amplifier. The mixer system has a double sideband noise temperature of about 1500K including i.f. amplifier contributions.

As shown in Fig. 1, the junction is a Nb-Nb point contact with one side insulated from the waveguide in order for us to monitor the dc I-V curve. The helium bath is usually pumped to 1.4K to reduce ambient temperature Johnson noise and to obtain a large RI_c product (small Ω_p).

Care was exercised to minimize the external noise reaching the junction. The bias leads passed through broad band rf filters whose adequacy was verified by measurements of the step rounding on the I-V curves with a cooled attenuator in the waveguide. The resonant coupling limited the

frequency band over which the junction was efficiently coupled to room temperature radiation to ≈ 50 MHz at 36 GHz.

After a junction has been obtained, we apply a small amount of pump power and adjust the plunger for minimum zero-voltage current. This indicates a maximum rf current flow in the junction and a cavity resonance close to the pump frequency. Then the junction bias current is switched off and the pump power increased until the critical current is almost zero. This usually takes place for a pump level of the order of 10^{-7} W. Under these conditions, parametric oscillations were observed with the spectrum analyzer for most of our junctions. Depending on very fine adjustments of the plunger position and pump power, the spectrum of parametric excitations from the same junction takes various shapes as shown in Fig. 5. One general feature of these spectra is that they are always symmetric with respect to the pump frequency. This provides evidence for a four-wave parametric interaction with the frequency relationship $2\,\omega_p = \omega_s + \omega_i$. We also observed that the reflected pump power drops suddenly when the oscillations appear. This is shown in Fig. 6 for three different junctions. Oscillations appear at the discontinuity in the slope of the curve.

Although the onset of parametric oscillations suggests that the negative resistance of the junction exceeds the cavity loss, not all the junctions that oscillate show net gain for a small signal applied within the frequency range of the oscillations. This implies that the onset of an instability prevents the negative resistance of those junctions from being continuously adjustable by the plunger and pump power. Once in the oscillating regime, the small signal assumption is no longer valid and no

amplification can be observed. For some junctions such as the one shown in Fig. 7 however, we observe both parametric amplification with a net gain > 10 dB and a rise in the noise background. In Fig. 8 we show the spectrum of the microwave power reflected from the shorting switch (a) and from the junction (b). In the latter case the reflected pump power has decreased, the signal is amplified by 11 dB, and an idler of comparable strength has appeared on the other side of the pump. The gain was found to be linear for an input signal as large as 35 dB below the pump level. As the signal frequency is varied, the gain profile seems to correlate with the shape of the amplified noise as would be expected, since both depend on the frequency dependence of the parametric gain. The bandwidth of both effects is limited by the resonant circuit to approximately 50 MHz.

The long term stability of the parametric amplifier was limited by the sensitivity of the gain to the pump amplitude shown in Fig. 3 and the relatively poor stability of the pump source (and/or the junction). This instability prevented us from measuring the noise by alternately observing matched loads at different temperatures.

An estimate of the junction noise temperature was made from the amount of noise background in Fig. 8. The system noise analysis is made as follows: With the shorting switch closed, the double sideband system noise output at any frequency within the mixer bandwidth of ~ 2 GHz is proportional to

$$T_1 = 2\,T_R + 2\,T_A\,, \tag{8}$$

where T_R is the single sideband mixer noise temperature referred to a point in front of the switch, and $T_A = 300$ K is the antenna noise temper-

ature the receiver sees. Using matched loads at room and liquid nitrogen temperatures to replace the signal source, we measured $T_R = 3500\ K \pm 200\ K$. With the switch open, the junction sees a noise temperature $T_{eff} = \alpha T_A + (1 - \alpha)\ T_{av}$ at both the signal and the idler frequencies. Here α is the one-way power attenuation factor of the copper-plated stainless steel waveguide between the junction and the switch, and T_{av} is its average temperature. If we assume that the junction amplifies with single sideband gain G and noise temperature T_N, the total noise output of the mixer at the signal frequency is proportional to

$$T_2 = 2\ T_R + 2(1 - \alpha)\ T_{av} + \alpha\ G(T_N + 2\ T_{eff}) + \alpha\ T_{eff} \qquad (9)$$

There is a factor of 2 in front of $\alpha G\ T_{eff}$ since the junction amplifies the noise at both the signal and the idler frequency, and converts it to the signal frequency. The last term in Eq. (9) represents the other sideband of the LO received by the mixer which is assumed to be totally reflected from the junction. In a separate measurement, we obtained $\alpha = 0.74$ and $T_{av} = 123$ K, so that $T_{eff} = 254$ K[20]. From Fig. 8 we estimate the ratio T_2/T_1 between the two noise levels underneath the signal to be 3 dB, and the gain at the junction to be G = net gain (11 dB)$/\alpha^2$ = 13.6 dB. From these numbers, and the ratio of Eqs. (9) to (8), we find that the amplifier noise temperature T_N is consistent with zero. Perhaps the most significant uncertainty in our estimate of T_N arises from a standing wave pattern (USWR $\sim$ 1.5) in the long stainless steel waveguide between the shorting switch and the junction. It limits the accuracy of α and T_{eff} to $\pm$ 10 percent. Because of this effect, and because of the possibility of saturation, we can only place an upper limit of about 50 K on the noise temperature T_N of the parametric amplifier.

IV. DISCUSSION AND CONCLUSION

In this work we have demonstrated four-wave parametric oscillation and external gain at 36 GHz in an unbiased point contact junction. This result helps to support the idea that previous observations of amplification from an unbiased thin superconducting film resulted from Josephson effects.[21,22] Qualitative agreement has been obtained between theory and experiment in that the oscillation or gain occurs when $\Omega_p \approx 0.1$ and the zero-voltage current is suppressed nearly to zero. No parametric effect, except for the appearance of a small idler, was detected for pump power beyond the first zero of the zeroth step. Amplification was only observed below the first zero, in the range in which the simple nonlinear inductance model is valid. This is an apparent disagreement with the results in Fig. 3 which show significant negative resistance for pump current beyond the first zero of the zeroth step.

The variability of our gain observations on junctions with essentially similar I-V characteristics is difficult to understand quantitatively. Certain junctions, which are saturated by amplified internal (or external) noise show little or no gain for a small external signal, and show a high value of T_N. Other junctions behave as nearly ideal parametric amplifiers as discussed above. We can speculate that accidental (parasitic) resonances at frequencies close to multiples of ω_p could be sensitive to the point geometry. These could invalidate the assumptions of our model and contribute to the variability of the saturation effects.

It would be very desirable to make a theoretical study of the effects of noise on both the singly degenerate and the doubly degenerate amplifier. This could be done to a first approximation by adding Johnson noise in the

shunt resistance to the equivalent circuit in Fig. 2. Such calculations would allow a test of our speculations about the reasons for the absence of gain in the singly degenerate amplifier. They would also allow a detailed investigation of the noise saturation effect which is the most important barrier to serious device application of the point contact parametric amplifier.

We were prevented from including noise in our digital calculations by limitations in the available computer time. The most promising way to carry out such calculations appears to be with an improved analog simulator which could produce quantitatively accurate results when biased at zero voltage.

Chiao et al.[7] have obtained performance similar to that reported here, but in a much wider bandwidth. This is due to their use of a series array of junctions. Since it may be some time before series arrays are available with as large values of the product I_cR as are now available from single point contacts, we may speculate that their wide bandwidth is obtained only with some sacrifice in the maximum operating frequency.

ACKNOWLEDGEMENTS

The authors wish to thank N. S. Nishioka for his help in computer programming and J. H. Claassen and P. T. Parrish for many useful discussions. We also thank A. R. Kerr for pointing out an important factor in the noise temperature estimate.

REFERENCES

*Work supported by the U. S. Office of Naval Research.

†NASA Goddard Institute for Space Studies, 2880 Broadway, New York, NY 10025

1. C. C. Grimes, P. L. Richards, and S. Shapiro, Phys. Rev. Lett. 17, 431 (1966).

2. H. Kanter and F. L. Vernon, Jr., J. Appl. Phys. 43, 3174 (1972).

3. H. Ohta, J. Appl. Phys. 43, 5161 (1972).

4. D. G. McDonald et al., Appl. Phys. Lett. 18, 162 (1971).

5. Y. Taur, J. H. Claassen, and P. L. Richards, Appl. Phys. Lett. 24, 101 (1974);Appl. Phys. Lett. 25, 759 (1974).

6. H. Kanter and A. H. Silver, Appl. Phys. Lett. 19, 515 (1971); H. Kanter IEEE Trans. Mag-11, 789 (1974).

7. P. T. Parrish et al.,Rev. Phys. Appl. 9, 229 (1974); P. T. Parrish and R. Y. Chiao, Appl. Phys. Lett. 25, 627 (1974); M. J. Feldman et al., J. Appl. Phys. 46, 4031 (1975); R. Y. Chiao and P. T. Parrish, J. Appl. Phys. 47, 2639 (1976).

8. P. Russer, Archiv. Elektrisch, Uebertrag. 23, 417 (1969).

9. A. N. Vystavkin et al.,Radiotek, Elektron. 15, 2404 (1970); Rev. Phys. Appl. 9, 79 (1974).

10. N. F. Pedersen, M. R. Samuelsen and K. Saermark, Rev. Phys. Appl. 9, 223 (1974).

11. N. F. Pedersen, M. R. Samuelsen, and K. Saermark, J. Appl. Phys. 44, 5120 (1973).

12. C. K. Bak, B. Kofoed, N. F. Pedersen, and K. Saermark, J. Appl. Phys. 46, 886 (1975).

13. Y. Taur, P. L. Richards, and F. Auracher, Low Temperature Physics-LT13, Vol. 3, K. D. Timmerhaus, W. J. O'Sullivan and E. F. Hammel, Eds. (Plenum Press, New York, 1974) p. 276.

14. K. Saermark (private communication).

15. C. A. Hamilton, Rev. Sci. Instr. 43, 445 (1972).

16. C. K. Bak, Rev. Phys. Appl. 9, 25 (1974).

17. P. Penfield, Jr. and R. P. Rafuse, Varactor Applications (MIT Press, Cambridge 1962).

18. Due to symmetry, Eq. (2) has two possible steady-state solutions which can be written as f(t) and π-f(-t). The stability requirement $\overline{\cos\phi_o(t)} > 0$ is satisfied by one and only one of them. Every time the zero-voltage step goes to zero, $\overline{\cos\phi_o(t)} = 0$ and the solution must jump to the other branch to be physically acceptable.

19. Eventually, as $I_p \to \infty$, $\mathrm{Re}Z_{ss} = R$ and $|Z_{si}| = 0$.

20. Strictly speaking T_{av} is different when referring to the hot or the cold end of the waveguide. In our case, however, the attenuation is small and this effect can be neglected.

21. A. S. Clorfeine, Appl. Phys. Lett. 4, 131 (1964).

22. H. Zimmer, Appl. Phys. Lett. 10, 193 (1967).

FIGURE CAPTIONS

Fig. 1. The Nb junction mounted in the microwave cavity. The stub at $3\lambda_g/4$ in front of the junction was present at room temperature. In some experiments, the stub was taken out so that the cavity was formed between the plunger and the junction itself. A circular choke groove was cut in the Nb flange to minimize microwave leakage.

Fig. 2. Equivalent circuit of the microwave cavity. Here the $3\lambda_g/4$ impedance transformation has been performed. The inductor in series with the junction represents the Nb wires. It has a reactance between 50 and 100Ω at 36 GHz. The resistance comes from losses in the cavity other than the junction. It was estimated to be less than 1Ω from a cavity Q measurement with the junction shorted.

Fig. 3. Calculated curves of small signal parametric resistance versus pump current. Parametric amplification can take place if the value is more negative than the cavity resistive loss.

Fig. 4. Block diagram showing the experimental arrangement. Arrows indicate power flow. Pump and LO attenuators are not shown.

Fig. 5. Different spectra of parametric excitations obtained from the same junction without applied signal. The unresolved line (resolution 1 MHz) at the center is the reflected pump.

Fig. 6. Reflected pump power versus incident power for three junctions The data have been normalized to superimpose the linear regions at low power. Junctions with smaller R appear to show a steeper negative slope after the break.

Fig. 7. Static I-V curves of a junction which shows net gain. Picture (a) was taken without pump applied. The junction is slightly hysteretic. Picture (b) was taken when the zero-voltage current is suppressed by the pump to almost zero and small signal parametric gain is observed.

Fig. 8. (a) Spectrum of the microwave input to the junction. The small signal is to the right of the applied pump.

(b) Spectrum of the microwave power reflected by the junction. The pump level is the same in these two pictures. The spectrum analyzer resolution is 1 MHz.

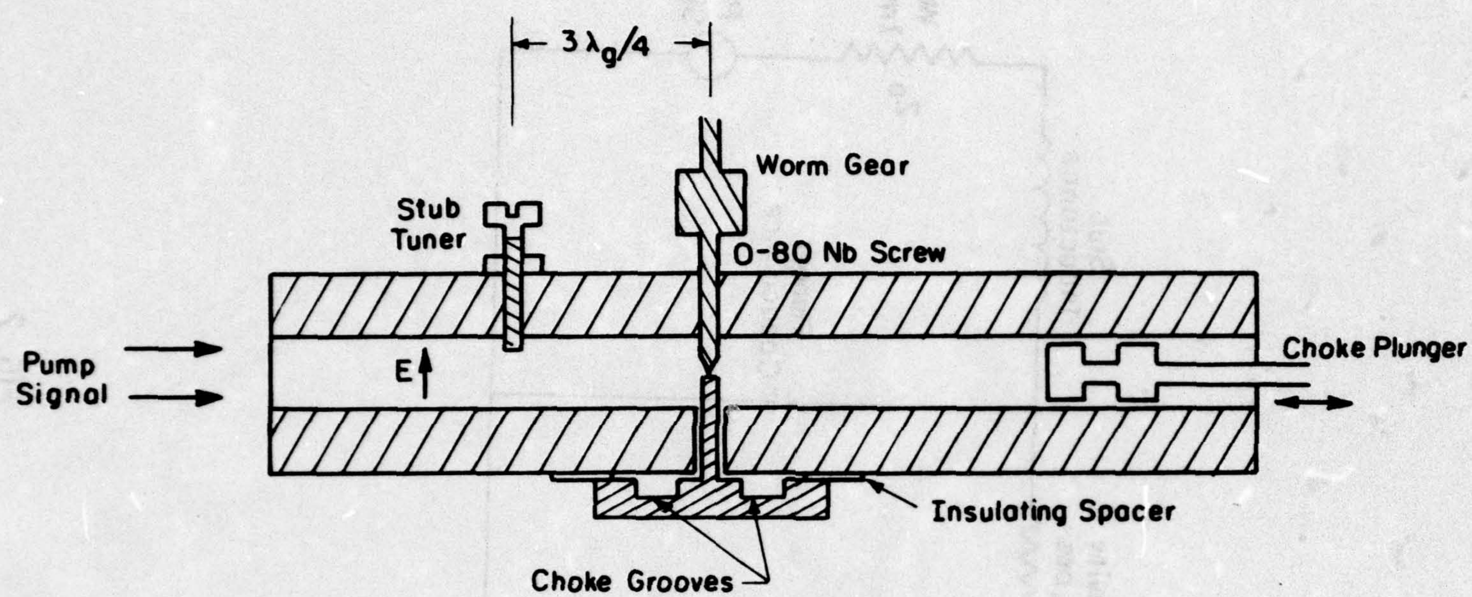
3 λg/4
Worm Gear
Stub
Tuner
0-80 Nb Screw
Pump
Signal
E
Choke Plunger
Insulating Spacer
Choke Grooves

FIG. 1

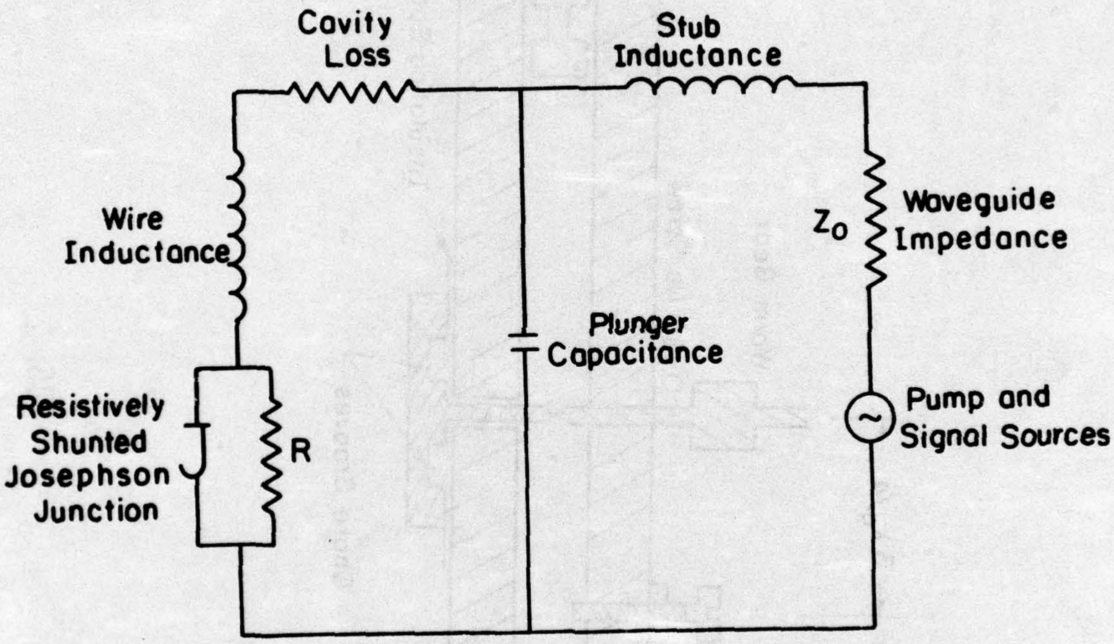
Cavity Loss
Stub Inductance
Wire Inductance
Waveguide Impedance
Z_0
Plunger Capacitance
Pump and Signal Sources
Resistively Shunted Josephson Junction
R

FIG. 2

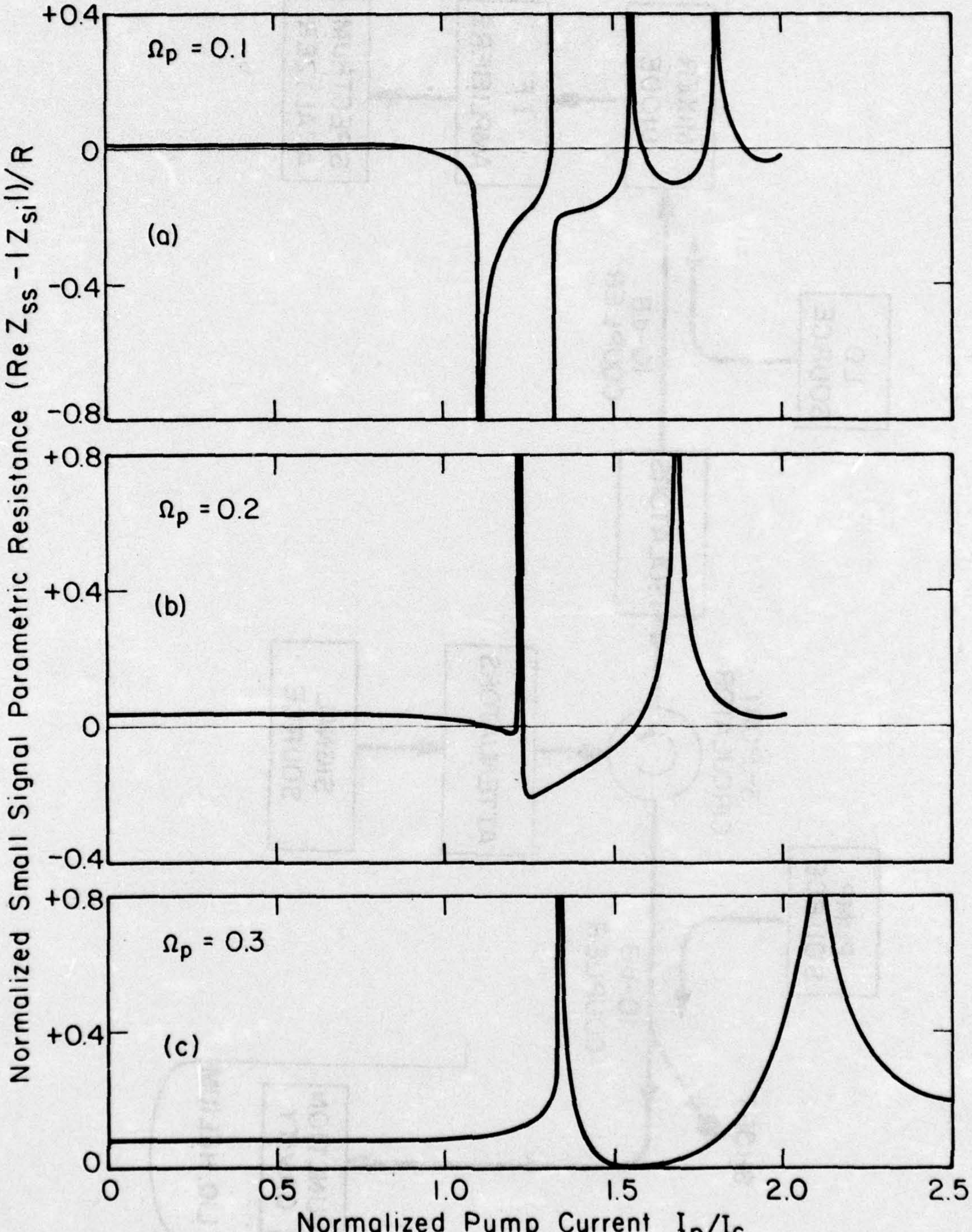

Normalized Small Signal Parametric Resistance (Re Z_ss - |Z_si|)/R
Ω_p = 0.1
(a)
Ω_p = 0.2
(b)
Ω_p = 0.3
(c)
+0.4
0
-0.4
-0.8
+0.8
+0.4
0
-0.4
+0.8
+0.4
0
0
0.5
1.0
1.5
2.0
2.5
Normalized Pump Current I_p/I_c

FIG. 3

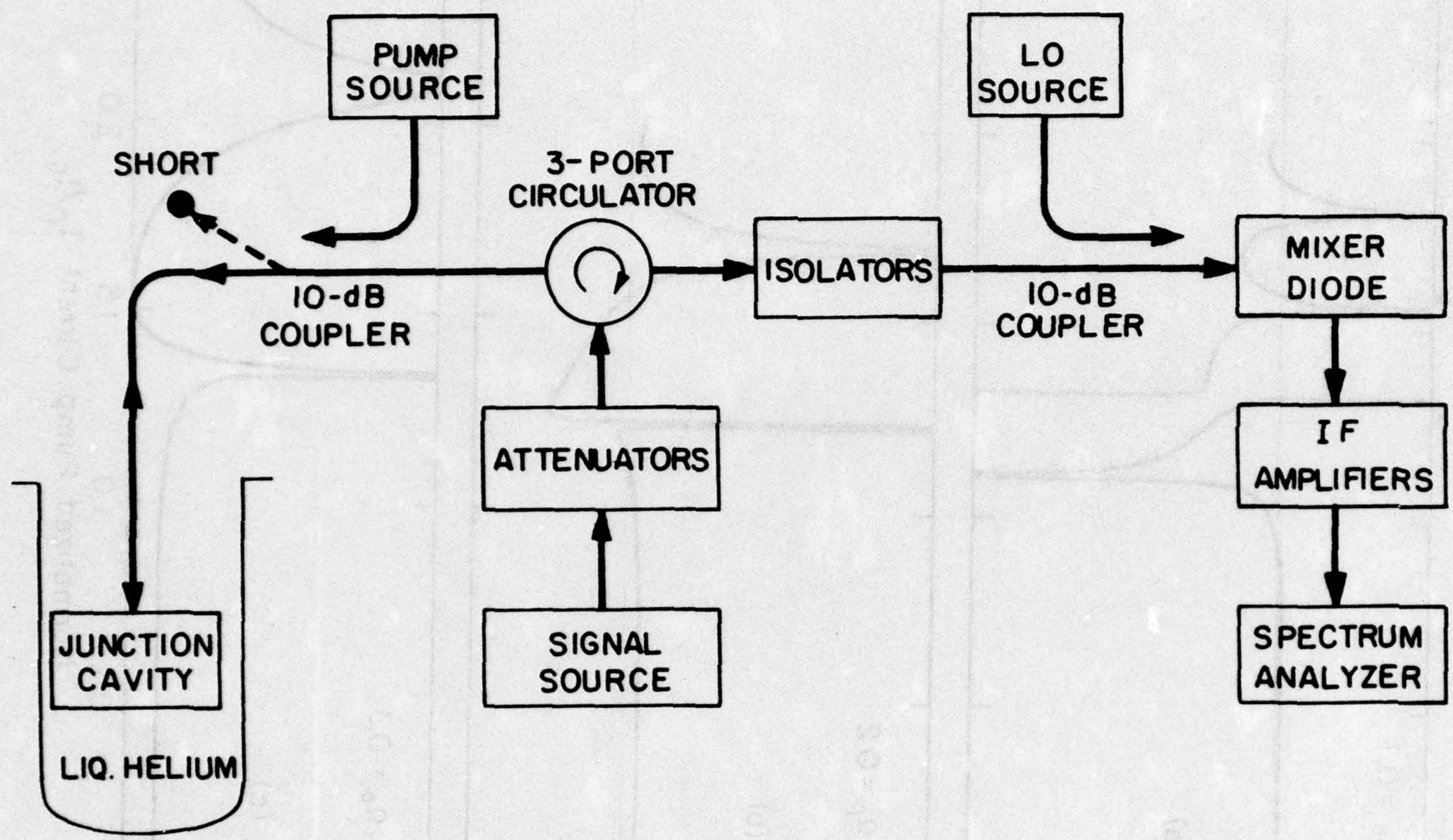
PUMP SOURCE
SHORT
3-PORT CIRCULATOR
LO SOURCE
ISOLATORS
10-dB COUPLER
MIXER DIODE
10-dB COUPLER
ATTENUATORS
I F AMPLIFIERS
JUNCTION CAVITY
SIGNAL SOURCE
SPECTRUM ANALYZER
LIQ. HELIUM

FIG. 4

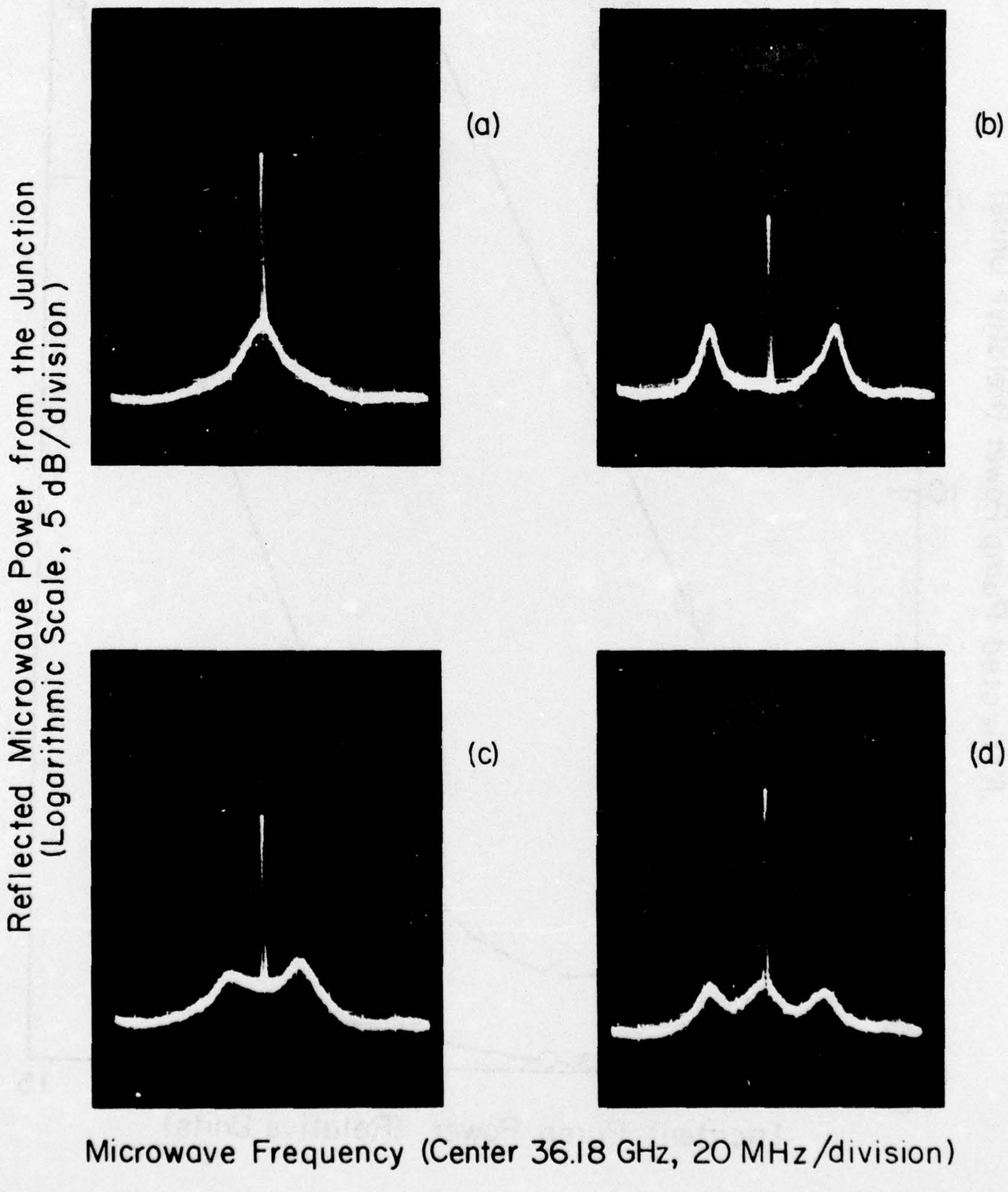

(a)
(b)
(c)
(d)
Reflected Microwave Power from the Junction
(Logarithmic Scale, 5 dB/division)
Microwave Frequency (Center 36.18 GHz, 20 MHz/division)

FIG. 5

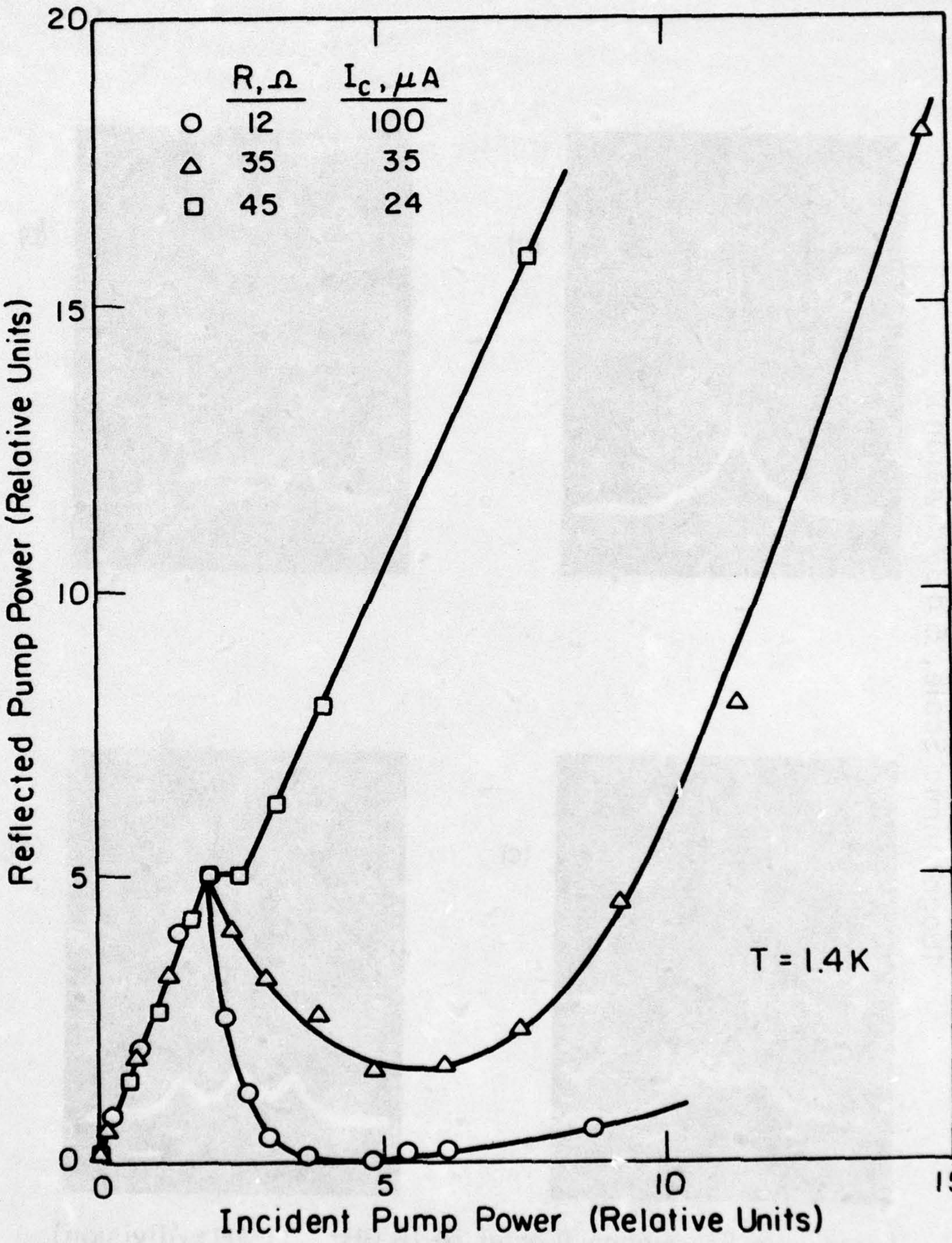

R, Ω
I_c, μA
12
100
35
35
45
24
T = 1.4K
Reflected Pump Power (Relative Units)
Incident Pump Power (Relative Units)
0
5
10
15
20

FIG. 6

Junction dc Current

(20 μA/division)

(50 μA/division)

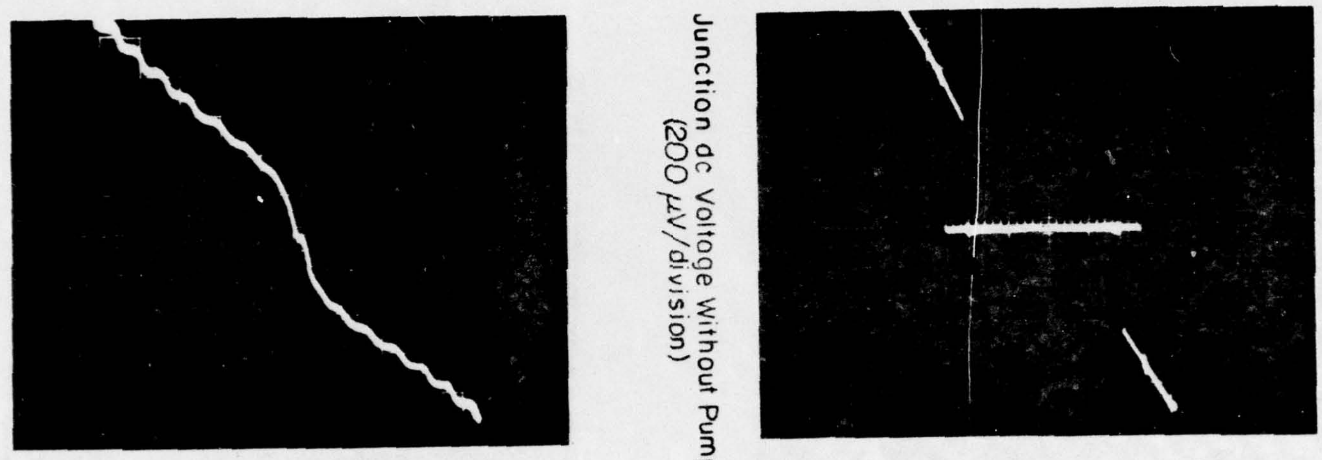

Junction dc Voltage With Pump
100 μV/division)

(b)

Junction dc Voltage Without Pump
(200 μV/division)

(a)

FIG. 7

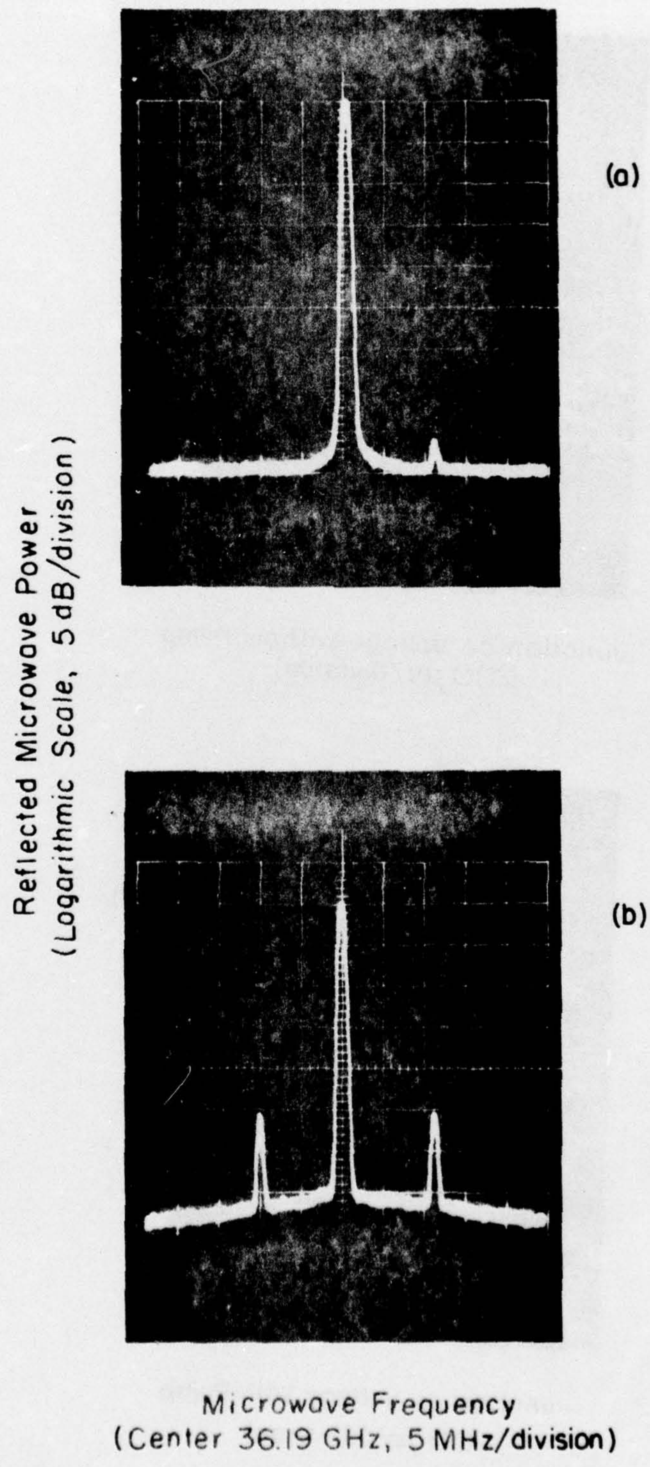
Reflected Microwave Power
(Logarithmic Scale, 5 dB/division)
(a)
(b)
Microwave Frequency
(Center 36.19 GHz, 5 MHz/division)

FIG. 8